RSC Advances

ROYAL SOCIETY OF CHEMISTRY

www.rsc.org/advances

Cite this: DOI: 10.1039/c0xx00000x

www.rsc.org/xxxxxx

ARTICLE TYPE

A facile label-free colorimetric aptasensor for ricin based on the peroxidase-like activity of gold nanoparticles†

Jingting Hu, [ab] Pengjuan Ni, [ab] Haichao Dai, [ab] Yujing Sun, [a] Yilin Wang, [ab] Shu Jiang, [ab] and Zhuang Li*[a]

Received (in XXX, XXX) Xth XXXXXXXXX 20XX, Accepted Xth XXXXXXXXX 20XX
DOI: 10.1039/b000000x

AuNPs possessed the peroxidase-like activity that could catalyze 3, 3, 5, 5-tetramethylbenzidine (TMB) in the presence of H_2O_2, leading to color change of the solution. Herein we propose a simple and sensitive colorimetric aptasensor for the quantitative analysis of ricin by using AuNPs. It is shown that the peroxidase-like activity of AuNPs can be improved by surface activation with target-specific aptamer. However, with target molecule, the aptamer is desorbed from the AuNPs' surface, resulting in a decrease of the catalytic abilities of AuNPs. The color change of the solution was relevant to the target concentration, and this can be judged by the naked eye and monitored by UV-vis spectrometer. The linear range for the current analytical system was from 0.05 nM to 10 nM. The corresponding limit of detection (LOD) was 0.05 nM. Some other proteins such as thrombin (Th), glucose oxidase (GOx), and bovine albumin (BSA) all had a negligible effect on the determination of ricin. What's more, several practical samples spiked with ricin were analyzed using the proposed method with excellent recoveries. This colorimetric aptasensor is superior to the other conventional methods owing to its simplicity, low cost, high sensitivity.

1.Introduction

Ricin is a highly toxic protein which is isolated from the seeds of castor bean Ricinus communis.[1] It is categorized as a type II ribosome inactivating protein, which contains a catalytic A chain with N-glycosidase activity and a lectin B chain assisting cellular uptake.[2,3] Ricin A chain is toxic to cells which inhibits the protein synthesis, thus leading to cell death. Ricin B chain is essential for binding to galactosyl residues on the cell surface and it is responsible for delivering the ricin A chain into the cell via endocytosis.[4,5] It is estimated that the LD_{50} for ricin in humans is approximately 5 to 10 μ g/kg through inhalation and there is no known antidote for it.[6]

Ricin has received significant attention since the infamous umbrella tip assassination of Georgi Markov demonstrated the extreme lethality of the toxin.[7,8] Recently， several terrorist groups have experimented with ricin and caused several incidents of the poison's being mailed to U.S. politicians. On May 29, 2013, two anonymous letters sent to New York City Mayor Michael Bloomberg contained traces of ricin. Another letter containing ricin was also alleged to have been sent to American President Barack Obama at the same time. Due to its ease of extraction in large quantities from castor beans, which are processed worldwide on an industrial scale, there is a real threat of ricin being used as a biological warfare agent. [9] Therefore， development of a rapid and sensitive detection method to monitor ricin has become more urgent.

Contemporary ricin detection methods are using such as Fourier transform near-infrared reflectance spectroscopy assay, [10] capillary electrophoresis assay,[11] surface-enhanced Raman spectroscopy [12] and antibody-based immunoassays.[13-19] Although, these assays are effective for ricin detection, most of these analytical methods rely on sophisticated instruments and skilled manpower, making such approaches impractical for on-site detection.

Of the alternatives to antibody-based sensing techniques, aptamer-based methods have become popular over the past decades due to their inherent selectivity, affinity, and multifarious advantages over the traditional recognition elements. As a new class of single-stranded DNA/RNA molecules, aptamers are selected in vitro by the systematic evolution of the ligand by the exponential enrichment (SELEX) process from random-sequence nucleic acid libraries. These molecular ligands have the ability to recognize their cognate targets with high affinity and specificity. This property makes aptamers an ideal tool to detect a variety of target molecules including proteins, drugs, small molecules, inorganic ions and even cells.[20-25]

Recently, increasing attention has been paid to the nanoscaled peroxidase mimetics and their potential applications in

[a]*State Key laboratory of Electroanalytical Chemistry, Changchun Institute of Applied Chemistry, Chinese Academy of Sciences, Changchun, Jilin 130022, PR China*
[b] *University of Chinese Academy of Sciences, Beijing, 100039, PR China*
Fax: +86 431 85262057; Tel: +86 431 85262057; E-mail: zli@ciac.jl.cn

† Electronic Supplementary Information (ESI) available:. See DOI: 10.1039/b000000x/

bioanalysis [26-31] since the first Fe_3O_4 magnetic nanoparticles-based peroxidase was reported. [32] A variety of nanomaterials have been also demonstrated to possess intrinsic peroxidase-like activity. Although gold is usually viewed as an inert metal, surprisingly it has been found that AuNPs possess intrinsic peroxidase-like activity.[33,34] The findings showed that a catalytic AuNPs-based strategy has enormous potentials in detection and can be exploited to develop biosensors for a wide variety of target analytes.

Enlightened by the above facts, we propose a colorimetric aptasensor for ricin based on the peroxidase-like activity of AuNPs. Rcin binding aptamer (RBA) could be absorbed onto the surface of AuNPs and improve the ability of AuNPs to catalyze 3, 3, 5, 5-tetramethylbenzidine (TMB) in the presence of H_2O_2 and lead to the significant enhancement of the absorbance. However, in the presence of ricin, the RBA undergoes target-responsive structural changes followed by desorption from the AuNPs surface to allow an aptamer-target binding event, resulting in a decrease in the catalytic abilities of AuNPs. The high selective and sensitive detection of ricin was possible using the naked eye or monitored by UV-vis spectrometer. Furthermore, the proposed method did not require any modification of the aptamer, making it time-saving and cost-effective.

2. Experimental

2.1. Reagent and chemicals

Ricin was purchased from Beijing Hapten and Protein Biomedical Institute (Beijing, china). The sequence of ricin binding aptamer (RBA) was 5'-ACACCCACCGCAGGCAGACGCAACGCCTCGGAGACTAG CC-3'. [35] The ssDNA oligonucleotides were synthesized by Shanghai Sangon Biotechnology Co. Ltd. (Shanghai, China) and the lyophilized powder was dissolved in distilled water and before use it was stored at 4 ℃. The concentration of the oligonucleotide was determined by measuring the UV absorbance at 260 nm. Chloroauric acid ($HAuCl_4$•$4H_2O$) was obtained from Shanghai Chemical Reagent Company (Shanghai, China). 3, 3, 5, 5-tetramethylbenzidine (TMB) and Hexadecyl trimethyl ammonium Bromide (CTAB) was purchased from Aladdin Reagent Company (Shanghai, China). Thrombin (Th), glucose oxidase (Gox), and bovine albumin (BSA) were purchased from Sigma-Aldrich Chemical Co (Milwaukee, WI, USA). $C_6H_5Na_3O_7$, H_2O_2, $Na_2HPO_4 \cdot 12H_2O$ and $NaH_2PO_4\ 2H_2O$ were obtained from Beijing Chemical Reagent Company. All of the reagents were analytic grade and used as received. Ultrapure water obtained from a Millipore water purification system (≥18 MΩ, Milli-Q, Millipore) was used in all runs.

2.2. Instrumentation

The ultraviolet-visible (UV-vis) absorption spectra were recorded on a Cary 50 Scan UV-vis spectrophotometer (Varian, USA) at 25℃. The zeta potentials were measured on Malvern Zetasizer Nanoseries at 25 ℃. Transmission electron microscopy (TEM) measurements were made on a Hitachi H-8100 transmission electron microscope operated at an accelerating voltage of 100 kV.

2.3. Synthesis of the citrate-protected AuNPs

AuNPs were synthesized using the classical citrate reduction method.[36] Briefly, colloidal AuNPs with an average diameter of 13 nm were prepared by rapidly injecting a sodium citrate solution (10 mL, 38.8 mM) into a boiling aqueous solution of $HAuCl_4$•$4H_2O$ (100 mL, 1 mM) with vigorous stirring. After boiling for 30 min, the reaction flask was removed from the heat to allow the reaction solution to cool at room temperature. The concentration of the AuNPs was about 10 nM, which was determined according to Beer's law by using the extinction coefficient of $2.78 \times 10^8\ M^{-1}\ cm^{-1}$ for 13 nm AuNPs in diameter at 520 nm. [37] The AuNPs was stored at 4 ℃ before use.

2.4. Detection of ricin using colorimetric biosensing method

A typical colorimetric analysis was realized as following procedure: first, 100 μL of 5 nM 13 nm AuNPs was mixed with 20 μL of 2.5 μM RBA. Second, 50 μL ricin with appropriate concentration in PBS (pH 7.4) was added to the AuNPs/RBA solution. The solutions were allowed to react for 5 min and then 15 μL of 6.7 mM TMB and 15μL of 6.7 M H_2O_2 were added to produce color change. The solution was equilibrated for 10 min at 25 ℃, and then was transferred to a quartz cuvette. The UV–vis absorption spectra were measured over the wavelength ranging from 400 nm to 800 nm.

2.5. Treatment of raw milk and Pepsi Cola

Milk samples were prepared following a previous method with a minor modification. [38] Briefly, 5.0 mL of raw milk was placed in a 7 mL centrifuge tube, and 1.5 mL of 2 M trichloroacetic acid was introduced. After ultrasonication for 10 min, the mixture was centrifuged at 10,000 rpm for 10 min. The Pepsi Cola was diluted 25 fold with PBS before use.

3. Results and discussion

3.1. The mechanism of the sensing system

Recently, it has been demonstrated that the peroxidase-like activity of nanoparticles varied with respect to electrostatic affinity between nanoparticles and substrates. Two substrates that would be helpful to evaluate this view.[39,40] ABTS （negatively charged）possesses two sulfonic acid groups, exhibiting high affinity toward a positively charged nanoparticle surface. With ABTS as the substrate, cationic nanoparticles displayed a high affinity and subsequently a high peroxidase activity. Conversely, TMB （positively charged） carries two amine groups, exhibiting strong affinity toward a negatively charged nanoparticle surface. With TMB as a substrate, anionic nanoparticles had a high affinity and exhibited a high catalytic activity.

As mentioned above, Fig. 1 outlines the concept of the catalysis-based colorimetric assay. According to previously reported,[41,42] a random coil ssDNA (RBA herein) could uncoil sufficiently to expose its bases, which could be easily adsorbed onto the surface of AuNPs. Thus, DNA phosphate backbone with a large number of negative charges existed on the surface of AuNPs. With positively charged TMB as a substrate, RBA-AuNPs complex had a high affinity and exhibited a significant enhancement of catalytic activity. However, when ricin was added, RBA bound to

ricin followed by desorption from surface of the AuNPs and the conformation of RBA was changed from random coil structure to G-quardruplex structure (rigid structure). The rigid structure prevented the exposure of the RBA bases to AuNPs and the negative charges existed on the surface of Au NPs became less, resulting in a decrease of the catalytic abilities of AuNPs.

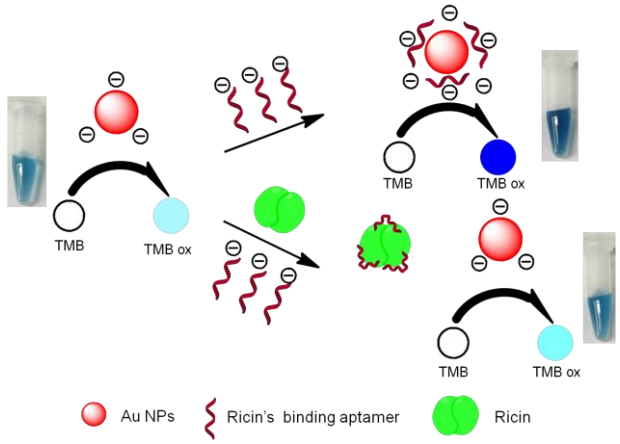

Fig. 1 The mechanism of the colorimetric aptasensor for ricin.

3.2. Spectral characteristics

To confirm the feasibility of our concept, the spectral responses of the colorimetric aptasensor were characterized under different conditions (Fig. 2A). The spectral value of AuNPs alone in solution at 650 nm was 0.98 absorbance units (a.u.) (1, Fig. 2A), explained by the oxidation of colorless TMB to blue TMB ox. In the presence of RBA, this value (2, Fig. 2A) increased to 1.5 a.u., indicating the enhancement of catalysis of AuNPs. When ricin molecules were present in the solution (3, Fig. 2A), RBA bound to ricin followed by desorption from the AuNPs, resulting in a decrease of the catalytic abilities of AuNPs. As expected, the addition of ricin alone did not cause the color change of the solution (4, Fig. 2A) compared with AuNPs alone (1, Fig. 2A). Further, the spectral value of AuNPs in the presence of CTAB (a kind of cationic surfactants) at 650 nm was 0.06 (5, Fig. 2A). These results confirmed that the negatively charged aptamer was the main cause of enhancement of AuNPs-dependent catalysis. Table 1 showed the Zeta potentials of AuNPs at different conditions and the results were in accordance with our mechanism.

In order to get rid of the possible impact of oxidation of TMB caused by RBA, ricin, and the ricin-RBA complex, these three molecules were also employed to the oxidation of TMB (Fig. 2B). The results indicated that RBA, ricin, and the ricin-RBA complex did not possess the peroxidase-like activity.

Fig. S1 showed the morphology characteristics of AuNPs under different conditions. The AuNPs were monodisperse and spherical with the average size of 13 nm (ESI, Fig. S1†). The UV-visible spectra of AuNPs, AuNPs-RBA, AuNPs-ricin and AuNPs-RBA-ricin complex showed a typical AuNPs SPR peaks with maxima at 520 nm, confirming the stability of AuNPs on different conditions (ESI, Fig. S2†). The observation showed that there was no aggregation of AuNPs caused by RBA, ricin and RBA-ricin complex.

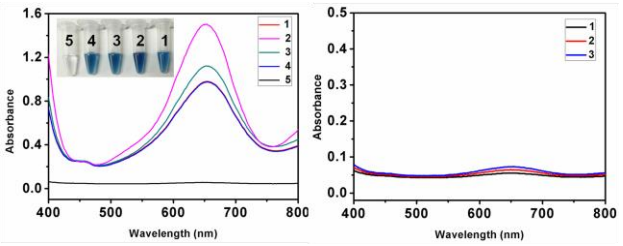

Fig. 2 (A) UV-vis spectra in the presence of TMB and H_2O_2 under different conditions of (1) 2.5 nM Au NPs, (2) 2.5 nM Au NPs + 0.25 μM RBA, (3) 2.5 nM Au NPs + 0.25 μM RBA + 0.5 nM ricin, (4) 2.5 nM Au NPs + 0.5 nM ricin, (5) 2.5 nM Au NPs + 0.5g/L CTAB. Inset shows the corresponding digital images. (B) UV-vis spectra in the presence of TMB and H_2O_2 under different conditions of (1) 0.25 μM RBA, (2) 0.25 μM RBA + 0.5 nM ricin (3) 0.5 nM ricin.

Table 1 Zeta potential of Au NPs under different conditions.

Sample	Zeta potential (mV)
AuNPs[a]	-14.9
AuNPs[a] + RBA[b]	-30.4
AuNPs[a] + CTAB[c]	4.9

[a] C_{AuNPs} = 2.5 nM, [b]C_{RBA} = 0.25μM, [c]C_{CTAB} = 0.5 g/L

3.3. Optimization of the key parameters

The peroxidase-like activity of AuNPs depends on some key parameters, such as the concentration of RBA, TMB and H_2O_2, reaction time and temperature. Therefore, these key parameters were optimized prior to the application of our proposed method. We used the reduction of absorbance, that is, A_0 - A (ΔA) as a criterion to optimize the detection conditions. A_0 presents the absorbance at 650 nm in the absence of ricin. A presents the absorbance at 650 nm in the presence of 0.5 nM ricin.

3.3.1. Effect of reaction time

Fig. S3 showed the effect of reaction time on the peroxidase-like activity of the sensing system. It was shown that the Δ A reach a platform from 10 to 20 min. Accordingly, 10 min was chosen as the reaction time. (ESI, Fig. S3†)

3.3.2. Effect of reaction temperature

Temperature is another crucial factor for most enzyme-based system. Fig. S4 showed that the ΔA increase with increasing temperature in the range from 15 ℃ to 25 ℃. Further increase in temperature resulted in the decrease of ΔA., Therefore, 25 ℃ was chosen as the reaction temperature. (ESI, Fig. S4†)

3.3.3. Effect of RBA concentration

Fig. S5 displayed the effect of RBA concentration of the sensing system. It is clear seen from Fig. S4, the concentration of RBA being too high or too low was not suitable for improving the Δ A. The ΔA reached the maximum value when the concentration of RBA was 0.25 μM. Hence, the concentration of RBA was selected to be 0.25 μM for this experiment. (ESI, Fig. S5†)

3.3.4. Effect of H_2O_2 and TMB concentration

The impact of TMB and H_2O_2 concentration on the Δ A were examined and shown in Fig. S6 and Fig. S7, respectively. It could be obviously seen that the maximum Δ A was obtained when the H_2O_2 concentration was fixed at 0.5 M and the TMB concentration was 0.5 mM. Therefore, 0.5 M of H_2O_2 and 0.5 mM of TMB was chosen for this experiments. (ESI, Fig. S6, Fig. S7†)

3.4. Colorimetric biosensing of ricin

Under the optimal detection conditions, the peroxidase-like of the AuNPs on TMB oxidation in the presence of various concentration of ricin was investigated. The ΔA at 650 nm in the presence of different amounts of ricin were shown in Fig. 3A. The digital images showed that with increasing ricin concentration, the color of the solution changed from dark blue to light blue, suggestive of the ricin concentration-dependent TMB catalysis. It could be evidently observed that the ΔA at 650 nm increase gradually with the increasing concentration of ricin. In another word, with the increasing concentration of ricin, the peroxidase-like acticities of AuNPs decreased. This observation is accord with our hypothesis. As shown in Fig. 3B,Δ A exhibited a good linear relationship with logC (ricin, nM) in the concentration range from 0.05 nM to 10 nM (R^2=0.9896). The detection limit can reach as low as 0.05 nM, which is lower than many previous reports. In addition, we compared the detection limit and detection time of the reported method. As shown in Table 2. The detection sensitivity of the proposed method is higher or comparable than the previous reports. Moreover, the detection time is much shorter than many previous reports. Most of the reported methods need tedious pretreatments while our method did not need them. Therefore, our method is simple and convenient.

Moreover, in order to investigate the stability of the sensor, we compared with the UV-vis spectra of fresh prepared AuNPs and aged AuNPs. (Fig. S8A) The UV-visible spectra of the two samples both exhibited a typical AuNPs SPR peaks with maxima at 520 nm, and the absorbance made no obvious differences between two samples. The results showed that AuNPs was stable even one month later. Further, we compared the performance for colorimetric biosensing between fresh prepared AuNPs and aged AuNPs. (Fig. S8B) It was shown that there existed slight differences between the two samples. In view of the above results, the sensor had a high stability. (ESI, Fig. S8†)

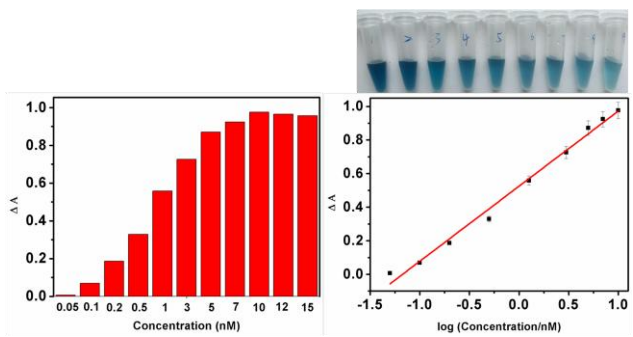

Fig. 3 (A) ΔA at 650 nm in the presence of various concentration of ricin. (B) Typical calibration curve for ricin obtained using the colorimetric aptasensor. Inset shows the corresponding digital images.

Table 2 Comparison of different method for ricin detection

Detection method	Detection Limit	Detection time (including Pre-treatment time)
Fluoroimmunoassay [43]	1000 ng/ml	12 h
Aptamer arrays biosensor assay [44]	320 ng/ml	6 h
SPR biosensor assay [45]	200 ng/ml	20 min
Immunochromatographic assay [18]	50 ng/ml	3 h
Aptamer- based SERS biosensor assay [46]	25 ng/ml	21 h
Aptamer-based colorimetric biosensor assay[47]	20 ng/ml	1 h
Microarray biosensor assay [48]	10 ng/ml	4 h
Nanoparticle-based colorimetric biosensor assay [19]	4 ng/ml	2 days
ELISA [49]	400 pg/m	20 h
Electrochemiluminescent assay [49]	50 pg/ml	11 h
Nanoparticle-based bio-barcode assay [50]	1 fg/ml	40 h
This work	**3.2** ng/ml	**1h**

3.5. Selectivity

The selectivity of this colorimetric aptasensor to ricin was evaluated by measuring the ΔA at 650 nm to some other proteins such as thrombin (Th), glucose oxidase (GOx), and bovine albumin (BSA). Fig. 4A showed that ΔA at 650 nm in the presence of ricin was considerably larger than those of other proteins. All results indicated that our assay approach had a high specificity to ricin.

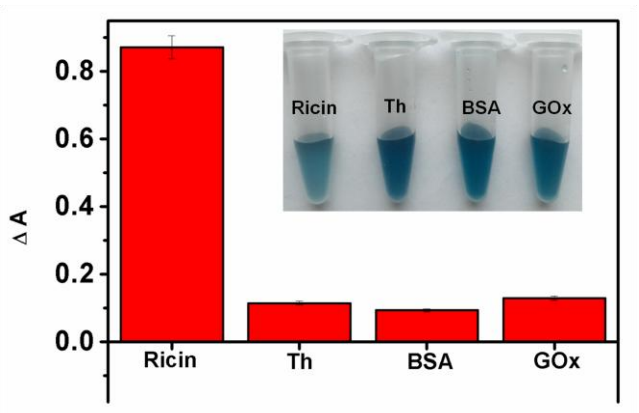

Fig. 4 The selectivity of the proposed system towards ricin detection. The concentration of ricin and other proteins are 7 nM. Inset shows the corresponding digital images.

3.6. Application in practical samples

In order to evaluate the feasibility of the present method in practical applications, the detection of ricin in raw milk and Pepsi Cola was carried out. The practical samples were spiked with certain amounts of ricin. Table 3 shows that the recoveries of the real samples are in the range 93.6% to 115.0%. The desirable recoveries demonstrate the reliability of the proposed method for detection of ricin in practical applications.

Table 3 Analytical results for ricin in raw milk samples and Pepsi Cola samples

Sample	Add (nM)	Found (nM) a	Recovery (%)	RSD (%)
Raw milk	1	1.15 ± 0.02	115.0	1.37
	8	8.24 ± 0.11	103.0	1.33
Pepsi Cola	1	0.94 ± 0.01	94.0	1.06
	8	7.49 ± 0.06	93.6	0.76

[a]Average of three determinations ± standard deviation

Conclusions

In summary, we have successfully developed a sensitive, accurate and reliable colorimetric aptasensor for the determination of ricin based on peroxidase-like activity of gold nanoparticles without complicated modification and expensive instruments. The color change of dark-blue to light-blue was found to be easily observed by the naked eye or measured by UV-vis spectrometer. The linear range for the current analytical system was from 0.05 nM to 10 nM. The corresponding limit of detection (LOD) was 0.05 nM. More importantly, the proposed method was successfully applied to the detection of ricin in practical samples. Therefore, this study may offer a new approach for developing simple, low cost and high sensitive sensors for ricin detection.

Acknowledgment

Financial support by the National Basic Research Program of China (973 program, no. 2010CB933600), the National Natural Science Foundation of China (21275135 and 21405146) is gratefully acknowledged.

References

1. L. M. Roberts and D. C. Smith, *Toxicon*, 2004, 44(5), 469–472.
2. J. M. Lord, L. M. Roberts and J. D. Robertus, *FASEB J*., 1994, 8 (2), 201−8.
3. J. Robertus, *Semin. Cell Biol.*, 1991, 2 (1), 23−30.
4. Y. Endo, K. Mitsui, M. Motizuki and K. Tsurugi, *J. Biol.Chem*., **1987**, *262*, 5908.
5. N. Sphyris, J. M. Lord, R. Wales and L. M. Roberts, *J. Biol. Chem*., **1995**, *270*, 20292.
6. L. L. He, B. Deen, T. Rodda, I. Ronningen, T. Blasius, C. Haynes, F. Diez-Gonzalez and T. P. Labuza, *J. Food Sci*., 2011, 76(5), N49–N53.
7. S. Olsnes, *Toxicon*, 2004, 44(4), 361–370.
8. M. Papaloucas, C. Papaloucas and A. Stergioulas, Pak. *J. Biol. Sci*., 2008, 11(19), 2370–2371.
9. K. Jasheway, J. Pruet, E. V. Anslyn and J. D. Robertus, *Toxicon*, 2011, 3, 1233–1248
10. L. E. Rodriguez-Saona, F. S. Fry and E. M. Calvey, *J. Agric. Food Chem*., 2000, 48(11), 5169–5177.
11. W. S. B. Yeung, G. A. Luo, Q. G. Wang and J. P. Ou, *J. Chromatogr. B*: *Anal. Technol. Biomed. Life Sci*., 2003, 797(1–2), 217–228.
12. L. L. He, B. Deen, T. Rodda, I. Ronningen, T. Blasius, C. Haynes, F. Diez-Gonzalez and T. P. Labuza, *J. Food Sci*., 2011, 76(5), N49–N53.
13. C. Lubelli, A. Chatgilialoglu, A. Bolognesi, P. Strocchi, M. Colombatti and F. Stirpe, *Anal. Biochem*., 2006, 355(1), 102–109.
14. E. A. E. Garber and T. W. O'Brien, *J. AOAC Int*., 2008, 91(2), 376–382.
15. N. Koja, T. Shibata and K. Mochida, *Toxicon*, 1980, 18(5–6), 611–618.
16. M. A. Poli, V. R. Rivera, J. F. Hewetson and G. A. Merrill, *Toxicon*, 1994, 32(11), 1371–1377.
17. U. Narang, G. P. Anderson, F. S. Ligler and J. Burans, *Biosens. Bioelectron.*, 1997, 12(9–10), 937–945.
18. R. H. Shyu, H. F. Shyu, H. W. Liu and S. S. Tang, *Toxicon*, 2002, 40(3), 255–258.
19. H. Z. Liu, J. J. Tang, X. X. Ma, L. Guo, J. W. Xie and Y. X. Wang, *Anal. Sci.*, 2011, 27(1), 19–24.
20. A. D. Ellington and J. W. Szostak, *Nature*, 1990, 346, 818–822.
21. T. Kunii, S. Ogura, M. Mie and E. Kobatake, *Analyst*, 2011, 136, 1310–1312.
22. J. Lee, M. Jo, T. H. Kim, J. Y. Ahn, D. K. Lee, S. Kim and S. Hong, *Lab Chip*, 2011, 11, 52–56.
23. R. L. Srinivas, S. C. Chapin and P. S. Doyle, *Anal. Chem*., 2011, 83, 9138–9145.
24. C. Tuerk and L. Gold, *Science*, 1990, 249, 505.
25. W. Yuanboonlim, W. Siripornnoppakhun, N. Niamnont, P. Rashatasakhon, T. Vilaivan and M. Sukwattanasinitt, *Biosens. Bioelectron*., 2012, 33, 17–22.
26. Y. Jv, B. Li, R. Cao, *Chem. Commun.*, 2010. 46 (42), 8017–8019.
27. S. Wang, W. Chen, A. Liu, L. Hong, H. Deng and X. Lin, *ChemPhysChem*., 2012. 13 (5), 1199–1204.
28. Z. Gao, M. Xu, L. Hou, G. Chen and D. Tang, *Anal. Chim. Acta*, 2013. 776, 79–86.
29. H. Jiang, Z. Chen, H. Cao and Y. Huang, *Analyst*, 2012.137 (23), 5560–5564.
30. X. Wang, Q. Wu, Z. Shan and Q. Huang, *Biosens. Bioelectron.*, 2011. 26 (8), 3614–3619.
31. J. Tian, Q. Liu, A. Asiri, A. Qusti, A. Al-Youbi and X. Sun, *Nanoscale*, 2013. 5 (23), 11604–11609.
32. L. Gao, J. Gao, L. Nie, J. Zhang, Y. Zhang, N. Zhang, T. Wang, J. Wang, D. Wang, S. Perrett, and X. Yan, *Nat. Nanotechnol*., 2007, 2 (9), 577 − 583.
33. M. Comotti, C. Della Pina, R. Matarrese and M. Rossi, *Angew. Chem., Int. Ed*., 2004, 43, 5812;
34. Y. Lin, Z. Li, Z. Chen, J. Ren and X. Qu, *Biomaterials*, 2013, 34, 2600.
35. J. J. Tang, J. W. Xie, N. S. Shao and Y. Yan, *Electrophoresis*, 2006, 27, 1303 − 1311
36. G. N. Mayer, *Nucleic Acid and Peptide Aptamers: Method and Protocols*. Humana, New York, NY, 2009.
37. M. M. Maye, L. Han, N. N. Kariuki, N. K. Ly, W. B. Chan,J. Luo and C.-J. Zhong, *Anal. Chim. Acta*, 2003, 496, 17 − 27.
38. X. F. Li, J. Li, H. Y. Kuang, L. Feng, S. J. Yi, X. D. Xia, H. W. Huang, Y. Chen, C. R. Tang and Y. L. Zeng, *Anal.Chim. Acta*, 2013, 802, 82 − 88.
39. F. Yu, Y. Huang, A.J. Cole and V.C. Yang, *Biomaterials*, 2009, 30, 4716–4722.
40. Y.P. Liu and F.Q. Yu, *Nanotechnology*, 2011, 22, 145704.
41. H. X. Li and L. J. Rothberg, Anal. Chem., 2004a, 76(18), 5414–5417
42. H. X. Li and L. J. Rothberg, J. Am. Chem. Soc., 2004b, 126(35),10958–10961.
43. G. P. Anderson and N. L. Nerurkar, *J. Immunol. Methods*,2002, (271), 17 − 24.
44. R. Kirby, E. J. Cho, B. Gehrke, T. Bayer, Y. S. Park, D. P. Neikirk, J. T. McDevitt and A. D. Ellington, *Anal. Chem*., 2004, 76, 4066 − 4075.
45. B. N. Feltis, B. A. Sexton, F. L. Glenn, M. J. Best, M. Wilkins and T. J. Davis, *Biosens. Bioelectron*., 2008, 23, 1131 − 1136.
46. E. A. Lamont, L. He, K. Warriner, T. P. Labuza and S. Sreevatsan, *Analyst*, 2011, 136, 3884 − 3895.

47. J. T. Hu, H. C. Dai, Y. J. Sun, P. J. Ni, Y. L. Wang, S. Jiang and Z. Li, *RSC ADV*., 2014, 4, 43998-44003.
48. J. B. Delehanty and F. S. Ligler, *Anal. Chem.*, 2002, 74, 5681 – 5687.
49. V. Guglielmo-Viret and P. Thullier, *J. Immunol. Methods*, 2007, (328), 70 – 78.
50. H. Q. Yin, M. X. Jia, S. Yang, S. Q. Wang and J. G. Zhang, *Toxicon*, 2012, 59, 12–16.

